Characterization of the Recognition of Tumor Cells by the Natural Cytotoxicity Receptor, NKp44†

Oren Hershkovitz,[#,‡] Sergey Jivov,[#,‡] Noga Bloushtain,[‡] Alon Zilka,[‡] Guy Landau,[‡] Ahuva Bar-Ilan,[‡] Rachel G. Lichtenstein,[§] Kerry S. Campbell,[∥] Toin H. van Kuppevelt,[⊥] and Angel Porgador*[,‡]

The Shraga Segal Department of Microbiology and Immunology, Faculty of Health Sciences, and the Cancer Research Center, Ben Gurion University of the Negev, Beer Sheva 84105, Israel, Department of Biotechnology Engineering, Ben-Gurion University of the Negev, Beer-Sheva, 84105, Israel, Division of Basic Science, Fox Chase Cancer Center, Philadelphia, Pennsylvania, and Department of Biochemistry, Radboud University Nijmegen Medical Center, NCMLS, Nijmegen, The Netherlands

Received January 10, 2007; Revised Manuscript Received April 19, 2007

ABSTRACT: NKp44 is a natural cytotoxicity receptor expressed by human NK cells upon activation. In this study, we demonstrate that cell surface heparan sulfate proteoglycans (HSPGs), expressed by target cells, are involved in the recognition of tumor cells by NKp44. NKp44 showed heparan sulfate-dependent binding to tumor cells; this binding was partially blocked with an antibody to heparan sulfate. In addition, direct binding of NKp44 to heparin was observed, and soluble heparin/heparan sulfate enhanced the secretion of IFNγ by NK92 cells activated with anti-NKp44 monoclonal antibody. Basic amino acids, predicted to constitute the putative heparin/heparan sulfate binding site of NKp44, were mutated. Tumor cell recognition of the mutated NKp44 proteins was significantly reduced and correlated with their lower recognition of heparin. We previously reported that NKp44 recognizes the hemagglutinin of influenza virus (IV). Nevertheless, the ability of the mutated NKp44 proteins to bind viral hemagglutinin expressed by IV-infected cells was not affected. Thus, we suggest that heparan sulfate epitope(s) are ligands/co-ligands of NKp44 and are involved in its tumor recognition ability.

Natural killer (NK)[1] cells are a highly specialized lymphoid population functionally identified by their potent cytolytic activity against tumor or virally infected cells (*1*). Their triggering is delicately regulated by a balance between opposite signals delivered by inhibitory and activating receptors (*2*). Detection of major histocompatibility complex (MHC) class I molecules on normal cells by the inhibitory receptors suppresses activation. On the other hand, expression of insufficient class I molecules, usually as a consequence of tumor transformation or viral infection, reduces the inhibition signal. The ground is then set for the triggering receptors to activate NK-mediated target-cell lysis (*2*−*8*). Three novel, NK-specific triggering surface molecules, NKp30, NKp44, and NKp46 (NCR3, NCR2, and NCR1, respectively) have been identified. These molecules represent the first members of a novel emerging group of receptors collectively termed natural cytotoxicity receptors (NCRs), all of which are capable of mediating direct killing of tumor and virus-infected cells and are specific for non-MHC ligands (*2*, *8*, *9*).

NCRs play an important role in recognizing and killing tumor cells. Therefore, elucidating the nature of the ligands recognized by NCRs is imperative. We have recently shown that membrane-associated heparan sulfate proteoglycans (HSPGs) are involved in the recognition of tumor cells by NKp30 and NKp46 (*10*). We further characterized the heparan sulfate binding site on NKp46 (*11*). Yet, the nature of the cellular targets recognized by NKp44 is still elusive. A cellular ligand for NKp44 was shown to be induced specifically on $CD4^+$ T cells from HIV-infected patients which correlated with a progressive loss of $CD4^+$ T cells (*12*). The recently published ternary structure of the NKp44 extracellular domain showed a positively charged inner surface of a prominent groove that may constitute a binding site for anionic ligands (*13*). Its existence suggests the possibility that heparin and heparan sulfate, which are negatively charged molecules, might be involved in the recognition of cellular targets by NKp44 as well.

† This study was supported by grants from the Israel Ministry of Health (MOH) and the Israel Cancer Research Foundation (ICRF). This work was also supported by the Cooperation Program of the Deutsches Krebsforschungszentrum (DKFZ) and Israel's Ministry of Science (MOS).

* To whom correspondence should be addressed. Tel: 972-8-647-7283. Fax: 972-8-647-7626. E-mail: angel@bgu.ac.il.

[#] These authors contributed equally to this work.

[‡] The Shraga Segal Department of Microbiology and Immunology, Faculty of Health Sciences, and the Cancer Research Center, Ben Gurion University of the Negev.

[§] Department of Biotechnology Engineering, Ben-Gurion University of the Negev.

[∥] Fox Chase Cancer Center.

[⊥] Department of Biochemistry, Radboud University Nijmegen Medical Center.

[1] Abbreviations: CD, circular dichroism; CHO, Chinese hamster ovary; GAG, glycosaminoglycan; HA, hemagglutinin; HN, hemagglutinin- neuraminidase; HRP, horse radish peroxidase; HSPG, heparan sulfate proteoglycans; IV, influenza virus; LIR-1, leukocyte immunoglobulin-like receptor-1; MFI, mean fluorescence intensity; MHC, major histocompatibility complex; NCR, natural cytotoxicity receptor; NK, natural killer; PFU, plaque forming units; PI, propidium iodide; RU, resonance units; SA, streptavidin.

10.1021/bi7000455 CCC: $37.00
Published on Web 05/31/2007

Table 1: Primers Used for Generating Point Mutations in NKp44-Ig[a]

Primers	Sequences
KpnI-fwd	GGCAGGGTACCCCAATCCAAGGCTCAGGTA
44/46-endseq	GCCGTCCACGTACCAGTTGAA
NKp44HRR3Afw	GCCTACTGGTGTGCCATCTACCGCCCTTCTGACAACTCTGTCTCTAAGTCCGTCGCCTTCTATC
NKp44HRR3Arev	GGCGACGGACTTAGAGACAGAGTTGTCAGAAGGGCGGTAGATGGCACACCAGTAGGCTCCTGAG
NKp44HRR3Qfw	CAGTACTGGTGTCAGATCTACCGCCCTTCTGACAACTCTGTCTCTAAGTCCGTCCAGTTCTATC
NKp44HRR3Qrev	CTGGACGGACTTAGAGACAGAGTTGTCAGAAGGGCGGTAGATCTGACACCAGTACTGTCCTGAG
NKp44RKR3Afw	GCCTTAGTCACCAGCTCCGCCCCCGCCACGATGG
NKp44RKR3Arev	GGCGGGGGCGGAGCTGGTGACTAAGGCGATGCACAC
NKp44RKR3Qfw	CAGTTAGTCACCAGCTCCCAGCCCCAGACGATGG
NKp44RKR3Qrev	CTGGGGCTGGGAGCTGGTGACTAACTGGATGCACAC

[a] Mutated codons are highlighted in gray.

In addition to the role of NCRs in immunity against transformed cells, they also contribute to the defense against other pathogens (*14*, *15*). We have previously reported that NKp44 and NKp46 proteins, but not NKp30, bind to hemagglutinin (HA) of the influenza virus (IV) and to hemagglutinin-neuraminidase (HN) of Sendai virus (*16*−*18*). The binding requires the sialylation of oligosaccharides on NKp44 and NKp46 and is also required for the lysis of virus-infected cells by NK (*16*, *17*).

In this study, we show that heparan sulfate is involved in NKp44-mediated IFNγ secretion from NK cells. We further show that NKp44 binds to tumor cells in a HSPGs-dependent manner and that NKp44 manifests direct binding to immobilized heparin. Finally, we partially characterize the heparin/heparan sulfate binding region in NKp44 by mutating the AA predicted to participate in the binding process.

MATERIALS AND METHODS

Cells and Viruses. Cell lines used in this work were as follows: PC-3, human prostate adenocarcinoma derived from bone metastasis that is PSA negative and Androgen insensitive (ATCC no. CRL-1435); 1106, human melanoma cell line established from a recurrent metastatic lesion and which expresses no HLA class I antigens (*19*); HeLa, human cervical adenocarcinoma (ATCC no. CCL-2); PANC-1, human pancreatic ductal carcinoma (ATCC no. CRL-1469) overexpressing glypican-1 (*20*). GAS6, PANC-1 cells stably transfected with full-length glypican-1 antisense construct, thus markedly reducing their glypican-1 expression at both the RNA and protein levels. Sham-PANC-1 are control-transfected PANC-1 cells, retaining high levels of glypican-1 (*20*). Wild-type CHO-K1 cells and the mutant derivatives CHO pgsA-745 and CHO pgsD-677 were kindly supplied by Dr. Jeff Esko and have been characterized in detail elsewhere (*21*). The NK-92 cell line, transduced by retrovirus to express high levels of wild-type NKp44 (designated as NK92−44), has been characterized in detail elsewhere (*22*). The IV A/PR/8/34 (H1N1) was in hen eggs.

Ig-Fusion Proteins. To generate NKp44-Ig, the sequence encoding the extracellular portion of NKp44 (accession number NM_004828, residues 1−169) was amplified by PCR from a cDNA isolated from human NK clones. The corresponding PCR fragment, containing a Kozak sequence and the leader sequence of CD5, was cloned into pcDNA3.1-Ig vector, encoding the CH2+CH3 regions of human IgG1 (*23*). To generate NKp44-Ig with HRR3A/3Q and RKR3A/3Q mutations, the external primer KpnI-fwd was used together with the internal complementary primers NKp44HRR3Arev, NKp44HRR3Qrev, NKp44RKR3Arev, NKp44RKR3Qrev, to create the PCR fragments HRR3A/Q left and RKR3A/Q left, respectively (Table 1). In the same way, the external primer 44/46-endseq was used together with internal complementary primers NKp44HRR3Afw, NKp44HRR3Qfw, NKp44RKR3Afw, NKp44RKR3Qfw, to create the HRR3A/Q right and RKR3A/Q right PCR fragments, respectively (Table 1). These fragments were mixed, denatured, and used again, as a template with the same external primers, to create four long fragments containing three point mutations HRR3A, HRR3Q, RKR3A, or RKR3Q. Sequencing of the constructs revealed that all cDNAs were in frame with the human Fc DNA. CHO cells were transfected with these expression vectors, and G418-selected clones were screened for highest protein production. Re-cloned high producer clones were grown in BIO-CHO-1 medium (Biological Industries, Kibbutz Beit Haemek, Israel), supernatants were collected daily and purified on protein-G columns using FPLC. SDS−PAGE analysis revealed that all Ig-fusion proteins were approximately 95% pure and of the proper molecular mass. The generation of LIR1-Ig fusion protein was previously described (*24*).

Glycosaminoglycans (GAGs). Low molecular weight heparin (LMW heparin) (H-3400), sodium salt heparin (H-4784), heparan sulfate (H-9902), hyaluronic acid (H-5388), chondroitin sulfate A (C-8529), and chondroitin sulfate C (C-4384) were purchased from Sigma, St. Louis, MO. In addition to heparan sulfate purchased from Sigma, heparan sulfate kindly provided by John T. Gallagher, was also used.

Flow Cytometry and Antibodies. Cells were incubated with indicated micrograms of various fusion-Igs for 2 h at 4 °C,

washed, and stained with FITC-conjugated-F(ab′)$_2$-goat-anti-human-IgG-Fcγ (109-096-098) or APC-conjugated-F(ab′)$_2$-goat-anti-human-IgG-Fc (109-136-098), Jackson ImmunoResearch, West Grove, PA. Staining and washing buffer consisted of 0.5% (w/v) BSA and 0.05% sodium azide in PBS. Staining of CHO and mutant CHO cells was performed with 2% FCS instead of bovine serum albumin (BSA) in the different buffers. Propidium iodide (PI) was added prior to reading for exclusion of dead cells. Flow cytometry was performed using a FACSCalibur flow cytometer (Becton Dickinson, Mountain View, CA). Data files were acquired and analyzed using BD CELLQuest 3.3 software. Fluorescence data was acquired using logarithmic amplification and reported fluorescence intensity units represent conversion of channel values according to the logarithmic scale (range 10^0 to 10^4). Results are shown either as staining histograms (X-axis represents fluorescence intensity and Y-axis represents cell counts) or as the geometric mean fluorescence intensity (MFI) of the stained populations. Geometric mean of the fluorescence intensities is recommended by BD for comparing relative fluorescence intensities between logarithmically acquired samples. For most binding inhibition experiments, fusion-Igs were premixed with the GAG and added to the cells for staining as above. When results are presented as MFI, average MFI $\pm$ SD of the duplicate staining is brought to show consistency of staining procedure. Human IgG1 (hIgG1 kappa, PHP010) was purchased from Serotec, Oxford, UK. AO4BO8 is a phage-display Ab that recognizes heparan sulfate; MPB49V is a phage-display Ab that does not recognize heparan sulfate and was employed as negative control for AO4BO8. Production of these Abs and their staining protocol has been previously described (*25*).

Glycosidases and Treatment of Cells. Tumor cells (10^6) were washed twice in PBS, resuspended in 1 mL of reaction buffer alone (mock treatment) or reaction buffer containing one of the following GAG-degrading enzymes (Sigma): keratanase (1 U/mL, K-2876), heparin lyase I (1.5 U/mL, H-2519), and heparin lyase III (1.25 U/mL, H-8891). Reaction buffer consisted of 1% (w/v) BSA, 1 μg/mL leupeptin, and 10 U/mL aprotinin in PBS. Cells were incubated with enzyme for 60 min at 37 °C, washed twice with PBS, and stained with fusion-Igs as above.

Direct Heparin Binding Assay. (i) Forward ELISA: plates were coated overnight at 4 °C with 4 μg/mL of various fusion proteins and hIgG1 (diluted with PBS, final volume 75 μL). Blocking buffer (PBS supplemented with 0.05% Tween 20 and 2.5% dry skim milk, 150 μL/well) was applied for 2 h, after which plates were washed with PBS with 0.05% Tween 20 (PBST) and incubated with 1 μg/mL heparin-biotin sodium salt (Sigma) for 1 h at 37 °C (100 μL/well). Following washing with PBST, 100 μL/well of Streptavidin-HRP was added for 30 min at 1:2000 dilution in PBST supplemented with 0.5% skim milk. Following washing with PBST, 100 μL/well of TMB was added and color was allowed to develop at room temperature in the dark. Optical density was read at 650 nm (Dynex Technologies MRX Microplate reader).

(ii) Backward ELISA: plates were coated with 4 μg/mL of streptavidin (diluted with PBS, final volume 75 μL) overnight at 4 °C. Blocking buffer (as above) was applied for 2 h, then plates were washed with PBST and 1 μg/mL heparin-biotin sodium salt was added for 1 h at 37 °C (100 μL/well). Following washing with PBST, 4 μg/mL of various fusion proteins and hIgG1 (diluted with PBST supplemented with 0.5% skim milk) were added for 1 h at 37 °C (100 μL/well). Following washing with PBST, HRP-conjugated goat anti-human IgG, Fcγ fragment-specific (Jackson), was added at a dilution of 1:5000 for 30 min. After washing and addition of TMB, plates were analyzed as described and background levels (i.e., with no heparin-biotin) were subtracted. To determine the point of saturation, backward ELISA was performed with titrated concentrations of NKp44 and LIR1 fusion proteins (0−60 μg/mL); HRP-conjugated goat anti-human IgG, Fcγ fragment specific, was added at a dilution of 1:1000 and was not a limiting factor. To assess blocking capacity of soluble GAGs, backward ELISA was performed as above with a 5 μg/mL concentration of NKp44-Ig that was preincubated with titrated concentrations of the different GAGs for 20 min at 4 °C.

BIAcore. BIACORE 3000 (BIACORE AB, Uppsala, Sweden) was used for studying the interactions between heparin and NKp44. Heparin-biotin (Sigma, 20 μg/mL) was immobilized on a streptavidin (SA) chip (BIACORE AB) in 0.1 M sodium acetate pH 3.0, using HBS buffer (10 mM Hepes pH 7.4, 150 mM NaCl, 3.4 mM EDTA and 0.005% Tween 20) as a running buffer. The flow rate used was 10 μL/min.

The immobilization response was 50 resonance units (RU). Then, all experiments were performed at a flow rate of 20 μL/min in HBS buffer at 25 °C. Different analyte concentrations (0, 78, 156, 312, 625, and 1250 nM) were injected, each followed by regeneration of the surface using 2 M NaCl with 20 mM NaOH. Association time was 10 min, and dissociation time was 3 min. Data processing was done by BIA evaluation software 4.1 using the steady state affinity model. An empty flow cell was used as a control and was subtracted from the responses obtained from the reaction surface. Residuals were below 1.5 RU (below 0.2%, supporting data online) and χ^2 was less than 1. The results were expressed in RUs against time or RU against concentration.

Circular Dichroism (CD) Analysis. NKp44 HRR3A/Q-Ig and NKp44 RKR3A/Q-Ig fusion proteins were analyzed for CD spectra at 0.330 and 0.495 mg/mL in 300 μL of PBS. CD analysis was done on a J-715 CD spectra instrument with a bandwidth of 1 nm, response time of 1 s, data pitch 0.2 nm, standard sensitivity, scanning speed of 20 nm/min, at room temperature, and at the range of 250−200 nm using a 1 mm path length cuvette. Each sample was measured fout times, and the average CD spectra were calculated automatically. Human NKp44-Ig and lysozyme proteins were chosen as a set of reference proteins.

Anti-NKp44 Activation of NK92-44. Plates (96U) were precoated with 0.05−0.2 μg/mL anti-NKp44 mAb (R&D SYSTEMS, MAB22491) for 3 h at 37 °C (diluted with PBS, final volume 100 μL). After 3 h at 37 °C, wells were washed three times with 200 μL of PBS before cells were added. While incubating the wells with the Ab, NK92−44 cells were preincubated in the experimental culture medium (supplemented with 20 U/mL human rIL-2 instead of 100 U/mL human rIL-2), supplemented with heparan sulfate or with chondroitin sulfate A (as control) for 2.5 h at 37 °C. A total of 4×10^4 NK92-44 cells/well in 200 μL of medium were incubated for 24 h at 37 °C. IFNγ concentrations in the supernatants were then assayed by standard ELISA according

to the manufacturer's instructions (BioLegend, San Diego, CA).

Binding of Fusion-Igs to IV-Infected Cells. 1106 melanoma cells (10^6/mL) were incubated overnight with 3×10^4 PFU of IV. Cells (infected or uninfected) were washed and stained with NCR-Igs as described above.

RESULTS

Elevated Secretion of IFNγ in the Presence of Heparan Sulfate by NK Activated with Anti-NKp44 mAb. We and others have shown that NKp30, NKp44, and NKp46 recognize a broad spectrum of tumors (*9*, *10*, *16*, *17*, *23*, *26*). We further showed that the membrane-associated heparan sulfate is involved in the recognition of cellular ligands by NKp46 and NKp30 (*11*, *27*, *28*). We speculated that NKp44 might recognize similar structures. The published ternary structure of NKp44 extracellular domain showed a positively charged inner surface of a prominent groove that may constitute a binding site for anionic ligands (*13*). The existence of this positively charged groove strengthened our assumption that heparin and heparan sulfate, which are negatively charged molecules, might be involved in the recognition of cellular targets by NKp44.

We first tested whether heparan sulfate might influence NK cell activation through NKp44. We employed NKp44-transfected NK-92 cells that express high levels of transfected wild-type NKp44 (designated as NK92-44) (*22*). NK92-44 cells were plated in wells that were precoated with an anti-NKp44 mAb. For some of the samples, the experimental culture medium was additionally supplemented with glycosaminoglycans (GAGs), either heparan sulfate or chondroitin sulfate A, at indicated concentrations. Twenty-four hours later, IFNγ concentration in the supernatants was assayed by standard ELISA (Figure 1). Incubation of NK92-44 cells with anti-NKp44 mAb resulted in IFNγ secretion while resting cells did not secret detectable IFNγ. Significant enhancement of IFNγ secretion was observed for mAb-activated NK92-44 cells co-cultured with heparan sulfate, but not with chondroitin sulfate A (Figure 1); this enhancement was correlated with increased concentrations of heparan sulfate. Enhanced IFNγ secretion following co-culture with heparan sulfate was observed for NK92-44 cells activated with either low (0.05 μg/mL) or high (0.2 μg/mL) concentrations of anti-NKp44 precoated wells (Figure 1A,B). However, anti-NKp44 activation was imperative, since co-culturing with heparan sulfate without anti-NKp44 did not induce IFNγ secretion by NK92−44 cells.

NKp44-Ig Binds to Heparan Sulfate on Tumor Cells. We next determined the involvement of cell membrane-associated GAGs in the binding of NKp44-Ig to its cellular ligands. We treated PC-3 tumor cells with (i) heparin lyase III, which efficiently degrades heparan sulfate with broad specificity, and (ii) heparin lyase I, which is selective in cleaving highly sulfated regions in heparan sulfate. Neither, however, degrades keratan sulfate or chondroitin sulfates A−E (*29*). We also treated tumor cells with keratanase, which efficiently degrades keratan sulfate, but not other GAGs. Treatment of PC-3 cells with heparin lyase I or III, but not with keratanase, reduced the binding of NKp44-Ig by 50% (Figure 2A). We also stained the cells with anti-heparan sulfate antibody HS4E4 (*25*) with similar results (Figure 2B).

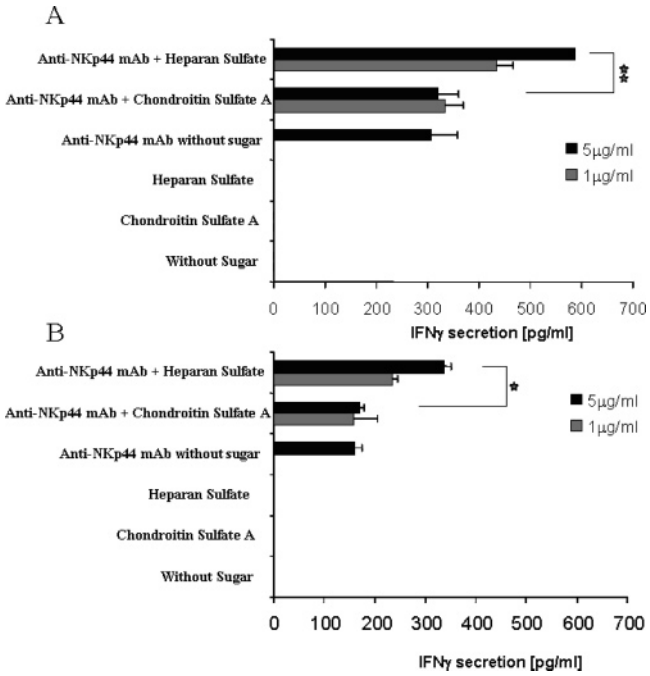

FIGURE 1: NK92−44 cells secrete higher levels of IFNγ in the presence of heparan sulfate after activation with NKp44 mAb. A total of 4×10^4 NK92-44 cells were incubated for 24 h in uncoated wells or wells precoated with anti-NKp44. Culture medium contained indicated concentrations (1 or 5 μg/mL) of either heparan sulfate or chondroitin sulfate A, or did not contain any GAGs. IFNγ concentrations in the supernatants were then assayed by standard ELISA. For antibody coating, 96 U-well plates were exposed to 100 μL of Anti-NKp44 mAb at 0.2 μg/mL (A) or 0.05 μg/mL (B) for 3 h at 37 °C. Wells were then washed twice with PBS, and cells were added. *$P < 0.004$ as analyzed by ANOVA single factor. **$P < 0.02$ as analyzed by ANOVA single factor. Results are from one representative experiment of four. Bars ± SD.

To further demonstrate the interaction of NKp44-Ig with cell surface heparan sulfate, we stained CHO mutants detected in GAG synthesis. Staining of CHO pgsA-745 cells, which have no heparan sulfate and chondroitin sulfate, with NKp44-Ig, was reduced by 60% compared to parental CHO-K1 cells (in MFI: 332 to 145) (Figure 2B1). A similarly reduced staining pattern was observed for CHO pgsD-677 (in MFI: 332 to 180) (Figure 2B1). The latter result was most revealing since CHO pgsD-677 cells have no heparan sulfate, but produce chondroitin sulfate that accumulates to levels 2−3 times higher than in the wild-type cells (*21*). In parallel, we stained CHO-K1 and CHO pgsA-745 with anti-heparan sulfate antibody HS4E4 (*25*). Staining with this antibody resulted in a similar pattern of staining (compared to staining with NKp44-Ig): MFI of 67 and 10 for CHO-K1 and CHO pgsA-745, respectively (Figure 2B3).

Next, we studied the glypicans involvement in NKp44 binding using the model of PANC-1. PANC-1 is a human pancreatic ductal carcinoma overexpressing the HSPG glypican-1 (*20*). GAS6 are PANC-1 cells stably transfected with full-length glypican-1 antisense construct, thus markedly reducing their glypican-1 expression. Consequently, GAS6 cells manifest reduced expression of membrane-associated heparan sulfate (data not shown). Sham-PANC-1 are control-transfected PANC-1 cells, retaining high levels of glypican-1 (*20*). We stained Sham-PANC-1 and GAS6 with NKp44-Ig. Staining of GAS6 was markedly reduced as compared to Sham-PANC-1 cells (in MFI: 463 to 89 for Sham-

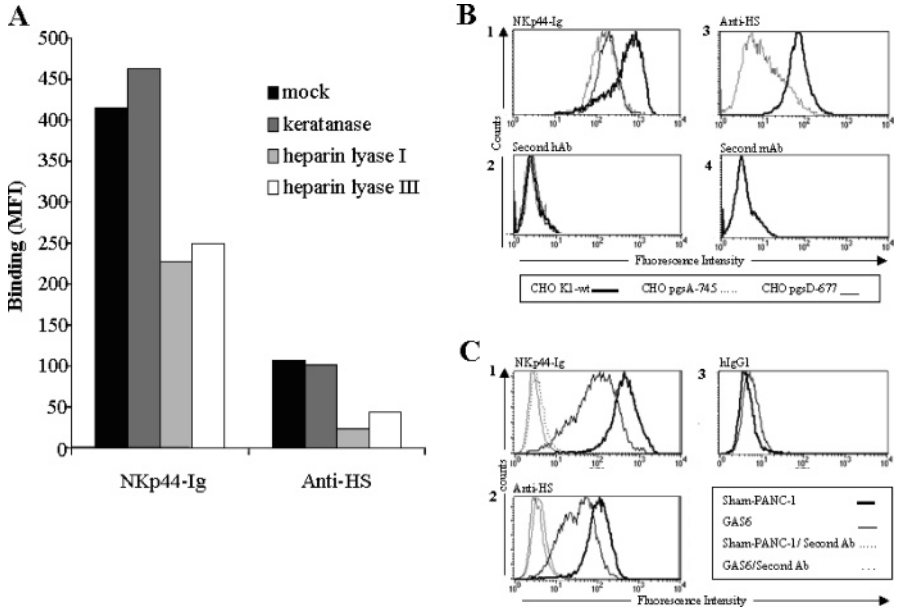

FIGURE 2: Effect of heparin-degrading enzymes, heparan sulfate deficiency, and glypican-1 suppression on binding of NKp44-Ig to tumor cells. (A) PC-3 cells were incubated in reaction buffer alone (mock treatment) or reaction buffer containing a GAG-degrading enzyme. After incubation, cells were washed and stained with NKp44-Ig and anti-heparan sulfate antibody HS4E4 (anti-HS). (B1, 2) Staining of parental CHO-K1, heparan sulfate-negative and chondroitin sulfate-negative CHO pgsA-745, and heparan sulfate-negative and chondroitin sulfate high-positive CHO pgsD-677 with NKp44-Ig (B1) or second Ab only (B2), (primary FACS histogram overlay). (B3, 4) Staining of parental CHO-K1 and CHO pgsA-745 with HS4E4 (B3) or second Ab only (B4). (C1, 2, 3) Staining of Sham and GAS-6 cells with NKp44-Ig, HS4E4, and hIgG1, respectively (primary FACS histogram overlay). Results are from one representative experiment of two. HS4E4 was used at a 1:16 dilution. For all panels, MFI results are the average of two samples assayed in the same experiment.

PANC-1 and GAS6, respectively) as shown in Figure 2C1. In the same experiment, we stained the cells with anti-heparan sulfate antibody HS4E4 (Figure 2C2). Staining with this antibody showed a similar pattern; reduction in staining of GAS6: MFI of 103 to 32 for Sham-PANC-1 and GAS6, respectively. Both cells showed similar low staining with human IgG1 (similar to background level; Figure 2C3).

Heparin/Heparan Sulfate Inhibits the Binding of NKp44-Ig to Tumor Cells. To further evaluate the involvement of heparin/heparan sulfate in the recognition of tumor cells by NKp44, we tested whether heparin can inhibit the binding of NKp44-Ig to tumor cells. HeLa cells were incubated with LMW heparin (10 μg/mL) and stained either with NKp44-Ig or with LIR1-Ig which is a NK fusion-Ig receptor used as a negative control. Heparin inhibited the binding of NKp44-Ig to HeLa cells but not the binding of LIR1-Ig (in MFI values: 491 to 110; Figure 3A). Chondroitin sulfate C did not inhibit the binding of both fusion proteins (Figure 3A). Similar results were obtained with 1106 melanoma cells (data not shown).

The specific role of heparin/heparan sulfate in competitive binding and consequent inhibition of NKp44-Ig binding to HeLa and PC-3 is further shown in Figure 3B. Incremental concentrations of chondroitin sulfate A, chondroitin sulfate C, and hyaluronic acid up to 100 μg/mL did not inhibit binding of NKp44-Ig. In contrast, LMW heparin and heparan sulfate in concentrations of 1 μg/mL (approximately 0.3 μM) inhibited binding of this fusion protein. Since the above results showed that the binding of NKp44-Ig to tumor cells was inhibited by heparin/heparan sulfate, we tested whether an antibody to heparan sulfate can inhibit NKp44-Ig binding to tumor cells. Preincubation of HeLa cells with AO4BO8, a heparan sulfate antibody previously described (*25*), suppressed binding of NKp44-Ig by almost 40%, while preincubation with an isotype control Ab (MPB49V), had no effect on NKp44-Ig binding (Figure 3C, inset). Dilutions of AO4BO8 antibody reduced its ability to inhibit NKp44-Ig binding to HeLa cells (Figure 3C). Antibodies that recognize diverse distinctive epitopes of heparan sulfate showed different abilities to competitively inhibit the binding of NKp44-Ig to tumor cells (data not shown).

Direct Binding of NKp44-Ig to Heparin/Heparan Sulfate. To demonstrate a direct interaction between heparin/heparan sulfate and NKp44, we used an in vitro binding system of the fusion proteins to their purified putative ligands on a solid matrix rather than on cell surface. We compared the binding of NKp44-Ig and hIgG1 to purified heparin in ELISA assays. Human IgG1 served as a control since the fusion-Igs contained the Fc portion of hIgG1. We used two complementary ELISA assays: binding the receptor (forward) or the ligand (backward) to the plate. In the forward assay, plates were coated with the different fusion-Igs. The plates were washed and biotin-tagged-heparin was added followed by SA-HRP. Results showed that NKp44-Ig binds directly to heparin when compared to the background recognition of hIgG1 (Figure 4A). In the backward assay, plates were coated with heparin and washed. Fusion-Igs were added, followed by HRP-conjugated goat anti-human Fc. Similar results were obtained in this assay (Figure 4B). We further determined the point of saturation in the backward ELISA: at the experimental conditions employed, 0.2 μM NKp44-Ig (20 μg/mL) saturated binding sites (Figure 4C). When preincubated with NKp44-Ig, incremental concentrations of soluble chondroitin sulfate C (up to 10 μg/mL) did not inhibit binding of NKp44-Ig to immobilized heparin. In contrast, soluble heparin and heparan sulfate, preincubated with NKp44-Ig, significantly inhibited its binding to the immobilized heparin (Figure 4D). These findings demon-

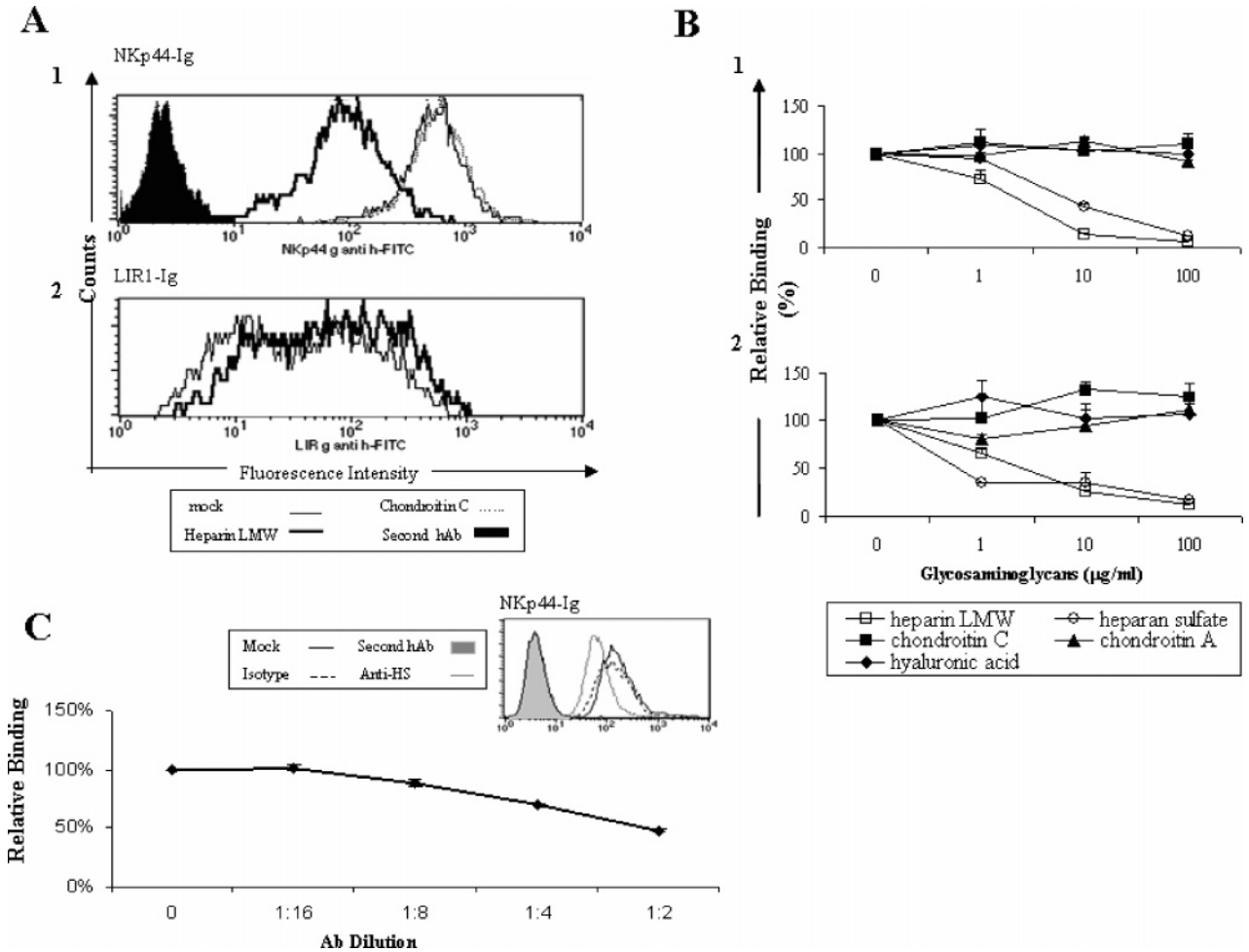

FIGURE 3: Effect of heparin/heparan sulfate on binding of NKp44-Ig to tumor cells. Fusion-Igs were premixed with different GAGs and exposed to 10^5 cells for 2 h at 4 °C. Heparan sulfate concentration of 1 μg/mL is approximately 0.3 μM. After incubation, cells were washed and incubated with FITC-anti-Fc secondary antibody. PI was added to exclude dead cells. (A) Staining of HeLa cells with NKp44-Ig (A1) and LIR1-Ig (A2) (primary FACS histogram overlays). LMW heparin and chondroitin sulfate C concentrations are 10 μg/mL. (B1, 2) Effect of titrated concentration of different GAGs on NKp44-Ig binding to HeLa and PC-3 respectively. (C) Effect of titrated AO4B8 on NKp44-Ig binding to HeLa cells. Diluted Ab was added to 10^5 cells for 1 h at 4 °C, before staining the cells with NKp44-Ig as described. Inset: primary FACS histogram overlay showing NKp44-Ig staining of HeLa cells preincubated with heparan sulfate antibody AO4B08 (diluted 1:2, final Ab concentration, 25 μg/mL) and isotype control antibody MPB49V, or preincubated in staining buffer (Mock). Results are from one representative experiment of two (graph) and six experiments (overlay inset). For the graph, results are the average of two samples assayed in the same experiment. Bars ± SD (of the duplicate, indicating the consistency of the staining procedure). Results are presented as percentage of binding as compared to staining of cells with NKp44-Ig alone, without GAG premix. For panels B and C, results are the average of two samples assayed in the same experiment. Bars ± SD.

strated the direct interactions between NKp44-Ig and heparin and supported the inhibition results for tumor staining (Figure 3). Next, we studied the binding of NKp44 and heparin using a BIAcore analysis system. A comparison of NKp44-Ig and LIR1-Ig binding to biotin-heparin immobilized to a streptavidin sensor chip (50RU) is shown in Figure 5A. While NKp44-Ig displayed a characteristic binding curve to heparin, no significant interaction could be detected with the other proteins tested (Figure 5A; data not shown for hIgG1 and CD99-Ig). To estimate the affinity between heparin and NKp44, we injected increasing concentrations of NKp44-Ig (0−1250 nM) over immobilized heparin (Figure 5B). Equilibrium dissociation constant (K_D) value, calculated with BiaEvaluation software 4.1, was 4.36×10^{-8} M using the steady state affinity model ($\chi^2 = 0.98$).

Mutating the AA Predicted to Constitute the Heparin/Heparan Sulfate Binding Site of NKp44 and Characterization of the Mutated NKp44-Ig Proteins. Since heparin/heparan sulfate are highly negatively charged molecules, the binding site on NKp44 should exhibit a high positive surface potential. Cantoni and colleagues published the 3D structure of NKp44 ectodomain (*13*). They concluded that the NKp44 displays a markedly asymmetrical surface charge distribution. In particular, four basic residues, Arg47, His88, Arg92, and Arg106, line the inner groove surface. Such residue distribution results in a positive electrostatic field emanating from an elongated patch inside the groove, likely conferring anionic binding specificity to this region (*13*). Reconstruction of the electrostatic potential map indicated that two other positively charged amino acids (Lys53 and Arg55) contribute to the positive patch (data not shown). On the basis of these observations, we decided to mutate Arg47, Lys53, Arg55, His88, Arg92, and Arg106 into noncharged amino acids and to examine the effect of these mutations on heparin/heparan sulfate binding compared to the wild-type NKp44-Ig. Using mutated oligonucleotides we constructed four PCR fragments, each containing three point mutations in which Arg47, Lys53, and Arg55 or His88, Arg92, and Arg106 were

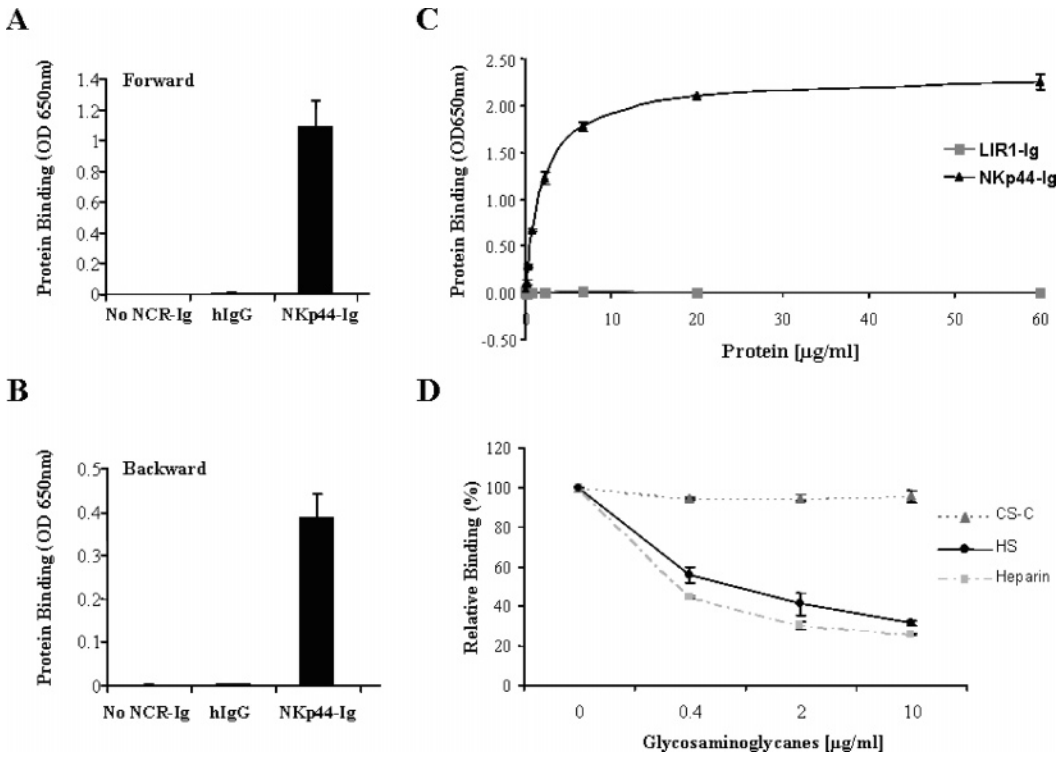

FIGURE 4: Direct binding of NKp44-Ig to heparin. (A) Forward assay: ELISA plates were coated with 4 μg/mL of NKp44-Ig and hIgG1, followed by incubation with 1 μg/mL biotin-tagged-heparin. Bound heparin was detected by SA-HRP. (B) Backward assay: ELISA plates were coated with 1 μg/mL heparin, followed by incubation with 4 μg/mL of fusion-Igs and hIgG1. Bound fusion-Igs were detected by HRP-conjugated anti-human Fc. (C) Titration of NKp44-Ig concentrations in the backward assay. Assay performed as above with incremented NKp44-Ig concentrations; HRP-conjugated goat anti-human IgG, Fcγ fragment-specific, was added at a dilution of 1:1000 and was not a limiting factor. (D) Blocking of soluble GAGs in the backward assay. Assay performed with 5 μg/mL concentration of NKp44-Ig preincubated with titrated concentrations of the different GAGs for 20 min at 4 °C. The data in (A−C) represent OD absorbance (650 nm). The data in (D) represent relative binding percentage normalized according to the binding of nonblocked NKp44. Results are from one representative experiment of two or three experiments. Results are the average of four samples assayed in the same experiment. Bars ± SD.

replaced by either glutamine or alanine (named RKR3Q/RKR3A or HRR3Q/HRR3A, respectively). Corresponding fusion proteins were prepared (designated NKp44/RKR3Q-Ig, NKp44/RKR3A-Ig, NKp44/HRR3Q-Ig, and NKp44/HRR3A-Ig) and compared to NKp44-Ig. AA sequences of NKp44 and the mutated fusion proteins at the putative heparan sulfate binding site are depicted in Figure 6A. SDS−PAGE analysis revealed that the integrity of the mutated fusion-Igs was not affected by the mutations, as presented in Figure 6B for NKp44/RKR3Q-Ig, NKp44/HRR3A-Ig, and NKp44-Ig. Qualitative MALDI analysis of NKp44-Ig and its mutants revealed the presence of monomeric fraction contamination (Figures 2−4 in Supporting Information). Yet, mutated NKp44-Ig fusion proteins did not exhibit higher monomeric fraction in the batches produced; Coomassie staining of NKp44-Ig and its mutants in SDS−PAGE gels in the presence (+) or absence (−) of β-mercaptoethanol showed none to very dull contamination of monomeric fraction (Figure 6 in Supporting Information). Next we applied circular dichroism (CD) analysis to revoke the possibility that the secondary structure of the mutated NKp44-Igs was distorted. The proteins were diluted in PBS to various concentrations and analyzed for CD spectra. Comparing the spectra of the NKp44-Ig to the other mutated NKp44-Igs showed a similar CD pattern, indicating that the secondary structure was not affected by the mutation. The CD spectra of NKp44-Ig, NKp44/RKR3Q-Ig, and NKp44/HRR3Q-Ig shown in Figure 6C has a similar CD spectra pattern, while the lysozyme protein used as a negative control showed a different spectra behavior. These results indicated that the biochemical characteristics of the mutated fusion proteins were similar to the wild-type protein. Yet, subtle changes to the secondary structure of the NKp44 protein are unlikely to be seen via the CD analysis. Therefore, for the next step of evaluation of heparan sulfate ligand recognition we also tested recognition of unrelated viral ligands by NKp44 and its mutants.

Binding of NKp44-Igs Mutants to Heparin/Heparan Sulfate, Tumor Cells, and Virus Infected Cells. To investigate the effect of NKp44 mutations on the direct interaction between heparin/heparan sulfate and NKp44, we employed the forward ELISA assay. Wells were coated with the different fusion-Igs and washed and biotin-tagged-heparin was added followed by SA-HRP. Without biotinylated heparin, wells coated with all fusion-Igs manifested insignificant background OD levels (Figure 7A). With biotinylated heparin added, NKp44-Ig, but not negative control LIR1-Ig, interacted well with the added heparin (Figure 7A). All NKp44-Ig mutants manifested only residual binding to added heparin (Figure 7A). Addition of non-biotinylated soluble heparin or heparan sulfate competitors, but not chondroitin sulfate, reduced binding of both NKp44-Ig and its mutants to the biotinylated heparin (data not shown). This indicates the specific nature of NKp44-Ig binding to heparin and that the NKp44 mutations tested suppressed, but did not abolish, NKp44 binding capacity to heparin/heparan sulfate.

We next studied the binding of NKp44 and its mutants to tumor cells and to IV-infected cells. We have previously

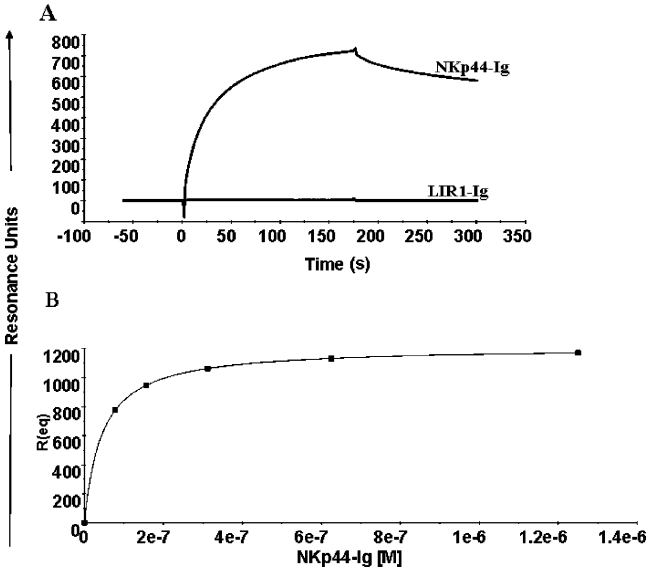

FIGURE 5: BIAcore analysis of NKp44/heparin interactions. The results from the BIAcore analysis are expressed in resonance units (RU) against time. Heparin-biotin was immobilized on a SA chip (50 RU). (A) NKp44-Ig and LIR1-Ig at 500 nM were injected over the heparin-immobilized surface. Curves show time-dependent specific binding after subtraction of background binding to the control flow cell (no heparin immobilized). The association time was 3 min followed by dissociation for 2 min (B) Evaluation of K_D for NKp44-Ig binding to heparin. NKp44-Ig was injected over heparin-immobilized surface at increasing concentrations, ranging from 0 to 1250 nM. The association time was 10 min, and the dissociation time was 3 min; data processing was done using the steady-state affinity model. Curve shows concentration-dependent specific binding after subtraction of background binding to the control flow cell. χ^2 was 0.98. Data represent one of five experiments performed and evaluated in different models.

shown that NKp44 recognizes the HA of IV and that this recognition improves the lysis of IV-infected cells (*17*, *23*). All the NKp44 mutants showed reduced binding to tumor cells, as compared to NKp44, and enhanced binding to IV-infected cells. The results obtained for NKp44/RKR3Q-Ig and NKp44/HRR3A-Ig mutants on 1106 melanoma cells and IV-infected 1106 cells are shown in Figure 7B. The negative control LIR1-Ig did not bind to 1106 cells and its binding was not enhanced following IV infection (Figure 7B). The binding of NKp44/RKR3Q-Ig and NKp44/HRR3A-Ig to 1106 melanoma cells was significantly reduced compared to NKp44-Ig and correlated with reduced recognition of purified heparin. However, enhancement of binding due to IV infection of 1106 cells was similar for NKp44 and its NKp44/RKR3Q-Ig and NKp44/HRR3A-Ig mutations (Figure 7B,C), indicating that mutations in the putative heparin/heparan binding site reduced the binding to the tumoral ligands but not to the viral HA ligand.

DISCUSSION

The cellular ligands recognized by NCRs are primarily expressed on cells upon activation, proliferation, or tumor transformation (*1*). Identification of the cellular ligands recognized by NCRs on tumor cells could pave the way for immunotherapy using NK cells, as well as the efficient targeting of tumor cells by mAbs specific for these ligands, or by using the recombinant NCRs themselves. We previously reported that membrane-associated HSPGs are involved in the recognition of cellular targets by NKp30 and NKp46 (*10*). In the current report, we further show that heparin/heparan sulfate is involved in the binding of NKp44 to tumor cells. Activation of NK92-44 cells with anti-NKp44 mAb in the presence of heparan sulfate, but not chondroitin sulfate, resulted in elevated secretion of IFNγ (Figure 1). Treatment of tumor cells with heparin lyase I/III but not keratanase reduced the binding of NKp44-Ig 2-fold (Figure 2A). Cells lacking heparan sulfate, but not chondroitin sulfate, were recognized to a lesser extent by NKp44 (Figure 2B). For PANC-1 cells, we demonstrated the involvement of a particular HSPG, glypican-1, in the recognition of tumor cells by NKp44, and this recognition correlated with membrane-associated heparan sulfate expression (Figure 2C). Therefore, the three NCRs (NKp30, NKp46, and NKp44) recognize epitope(s) expressed on the heparan sulfate component of HSPGs. The reduced recognition by NCRs of CHO cells lacking membrane-associated heparan sulfate and glypican-1-suppressed pancreatic cancer cells directly correlated with reduced lysis of these targets by NK cells (*10*). Heparin/heparan sulfate but not any other tested GAGs were able to inhibit the binding of NKp44-Ig to tumor cells (Figure 3A,B). In addition, the heparan sulfate antibody was able to partially block the NKp44-Ig binding to HeLa cells (Figure 3C). We demonstrated with ELISA measurements and BIAcore analysis a direct interaction between NKp44-Ig and heparin (Figures 4 and 5). These results corroborate the ternary structure of NKp44 extracellular domain (*13*), which reveal a positively charged inner surface of a prominent groove that might constitute a binding site for heparin/heparan sulfate.

Finally, we decided to mutate the positively charged Arg47, Lys53, Arg55, His88, Arg92, and Arg106, predicted to be involved in NKp44 binding to heparan sulfate (*13*), into noncharged amino acids. NKp44-Ig mutants were generated, each containing three point mutations either in Arg47, Lys53, and Arg55 or in His88, Arg92, and Arg106. Mutating these AA had no effect on the biochemical characteristics of the NKp44-Ig mutated proteins (Figure 6). Compared to the wild-type NKp44, the mutated proteins displayed reduced binding to purified heparin, which correlated with their suppressed ability to bind tumor cells as shown for NKp44/RKR3Q-Ig and NKp44/HRR3A-Ig mutants (Figure 7A,B). However, the mutated NKp44 proteins manifested enhanced binding to IV-infected cells (Figure 7B,C). Overall, the results support our initial prediction that these basic amino acids are involved in the binding of NKp44 to heparin/heparan sulfate.

The interaction of NCRs with heparan sulfate epitopes on HSPGs may facilitate the binding of the NCRs to other, hitherto elusive, cellular ligands. For example, the heparan sulfate epitope(s) may serve as co-ligands for the NCRs, similar to heparin/heparan sulfate interaction with either growth factors and growth factor receptors or with lipid binding proteins (*30*, *31*). Similarly, recognition of stromal cells by CD19, a coreceptor of the B-cell receptor, was shown to involve HSPGs expressed by the stromal cells (*32*). In this case, the heparan sulfate epitope(s) recognized by the NCRs could be similar (or even identical), while the primary cellular ligands, which are likely different for the three NCRs, explain the functional observations, indicating different specificities for the different NCRs (*1*, *9*). Yet, heparan sulfate exhibits a considerable number of unique overlapping sequences with peculiar sulfation profiles, and these se-

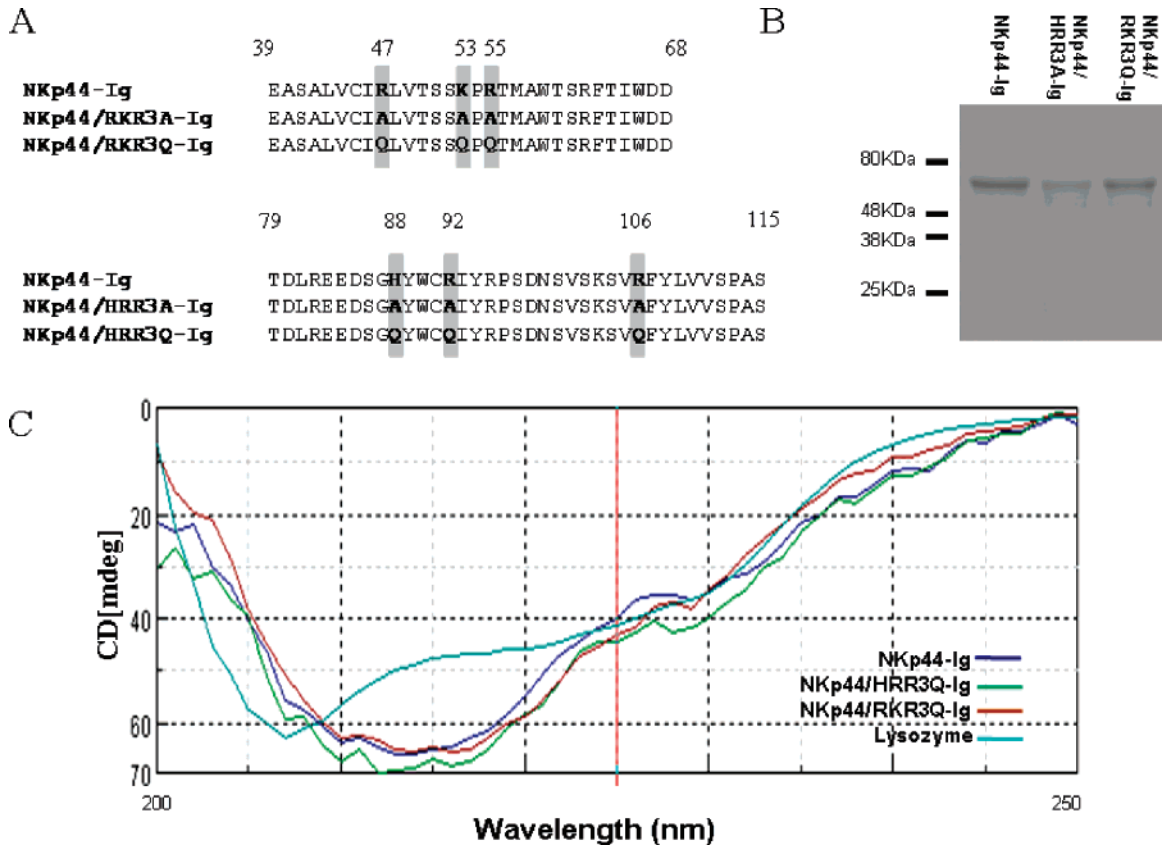

FIGURE 6: AA sequence and CD spectra of NKp44 and its mutations. (A) AA sequence of NKp44-Ig, NKp44RKR3A/Q-Ig, and NKp44HRR3A/Q-Ig at the putative heparan sulfate binding site. AA depicted are from 39 to 68 and from 79 to 115 for NKp44RKR3A/Q-Ig and NKp44HRR3A/Q-Ig, respectively, according to NKp44 extracellular domain aa numbering (*13*). (B) Sample proteins were separated on a 10% SDS−PAGE and Coomassie stained. Analysis has revealed that all mutant Ig fusion proteins were of high purity and the proper molecular mass as presented for NKp44RKR3Q-Ig and NKp44HRR3A-Ig. (C) Representative CD curves shown are for NKp44-Ig (dark blue), NKp44RKR3Q-Ig (red), NKp44HRR3Q-Ig (dark green), and control lysozyme (bright blue). The applied protein concentrations were 0.330 and 0.495 mg/mL in 300 μL of PBS. CD spectral analysis was performed in a J-715 with a bandwidth of 1 nm, response time of 1 s, data pitch 0.2 nm, standard sensitivity, scanning speed of 20 nm/min, at room temperature, at the range of 250−200 nm with a 1 mm cuvette. Results are from one representative experiment of two.

quences are recognized by specific complementary proteins (*33*). BIAcore-based consecutive injections of the different NCRs on immobilized heparin and under saturation conditions showed that the heparin epitopes recognized by NKp30 and NKp46 are indeed cross-reactive, yet the epitope recognized by NKp44 is different (A.P., unpublished results). Therefore, even though heparan sulfate could serve primarily as a co-ligand for NCRs' recognition, its recognized epitopes differ between NKp44 and NKp30/46.

Other than HSPGs as co-ligands, the identity of cellular/tumoral ligands to NCRs is still elusive. Recently, it was suggested that vimentin expressed on *Mycobacterium tuberculosis*-infected human monocytes is involved in binding to the NKp46 receptor (*34*). Enhanced recognition of mitotic cells by NK involved ligation of NKp44 and NKp46 as well as target-cell hyaluronan, another member of the GAG family. Yet, the authors could not show direct interaction between NKp46 and hyaluronan (*35*). Warren and colleagues reported that NKp30 does not bind to membranal heparan sulfate on target cells and that heparan sulfate is not involved in NKp30-mediated lysis (*36*). We examined the binding to membranal heparan sulfate of six different recombinant NKp30s, produced in different laboratories. We concluded that NKp30 does interact with membranal heparan sulfate (A.P., unpublished results). Indeed, the commercially available recombinant NKp30 (employed by Warren et al. (*36*)) did not show heparan sulfate-dependent binding. We demonstrated that this is due to an aberrant massive glycosylation of this recombinant NKp30 (A.P., unpublished results).

Our studies showed that all three NCRs bind tumors in a heparan sulfate-dependent manner (refs *10* and *11* and Figures 2 and 3) and that heparan sulfate serves as a co-ligand for NKp44-mediated IFNγ production by NK cells. However, the effect of heparan sulfate binding on NCR-mediated lysis is not clear (*10*, *36*). Recently, it was observed for NK−DC interactions that NKG2D and NCR recognition of their respective ligands is a prerequisite for IFNγ production but not for enhanced cytolysis (*37*). Similarly, NCR−heparan sulfate interaction could promote NK activation through IFNγ production but not through cytolysis enhancement. Alternatively, the presence of NK inhibitory receptors that recognize heparan sulfate as a co-ligand could explain the inconsistent results with regard to heparan sulfate−NCR-dependent cytolysis.

Alteration of the heparan sulfate epitope repertoire was observed both within various healthy tissues and between healthy and cancerous tissues (*25*, *38*). Therefore, tumor-modified heparan sulfate might overexpress certain existing epitope(s) or express separate unique carbohydrate epitopes (*39*, *40*) recognized distinctively by NCRs and rarely expressed on membrane-associated heparan sulfate on normal cells. In this scenario, the heparan sulfate epitope(s) recog-

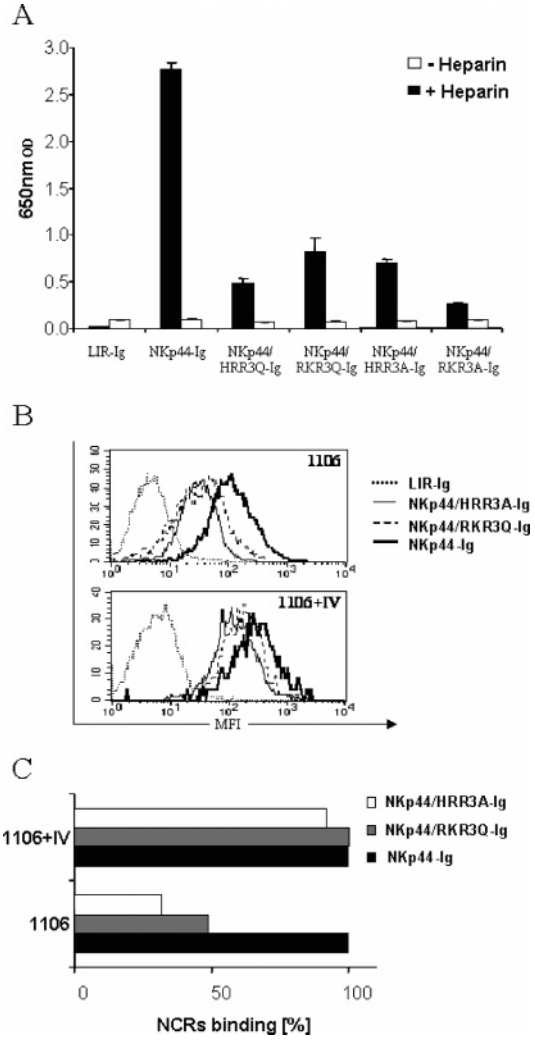

FIGURE 7: Binding of NKp44-Ig and NKp44-Ig mutants to heparin and to noninfected and IV-infected tumor cells. (A) ELISA plates were coated with 4 μg/mL of fusion-Igs, followed by incubation with 2 μg/mL biotin-tagged heparin. Bound heparin was detected using SA-HRP followed by TMB. The data in the figure represent OD absorbance (650 nm). Results are from one representative experiment of three and calculated as the average of three different samples assayed in the same experiment. Bars $\pm$ SD. (B−C) 1106 human melanoma cells were incubated overnight with IV (3×10^4 PFU to 10^6 cells). Cells (infected or uninfected) were washed, incubated with fusion Igs for 2 h, and stained with APC goat-anti-human. PI was added to exclude dead cells. (B) Overlay diagram of a representative experiment compares the binding of NKp44-Ig with HRR3A-Ig, RKR3Q-Ig, and LIR-Ig. (C) Normalized quantification of the binding of NKp44-Ig and its mutants to 1106 and IV-infected 1106 cells depicted in B. For 1106 cells: NKp44-Ig binding (MFI value) was normalized to 100% and NKp44 mutant binding was normalized accordingly. For IV-infected cells: enhancement (MFI values) of NKp44-Ig binding to IV-1106 compared to 1106 was normalized to 100%. Enhancement of NKp44 mutants binding to IV-1106 compared to 1106 was normalized accordingly. Results are from one representative experiment of three.

nized by the different NCRs could be tumor-related. If unusual heparan sulfate epitopes on cancer cell membranes lead to better signaling through growth factor receptors, it might be that NK-expressed NCRs evolved to recognize and penalize the uncommon epitope-expressing transformed cells. If so, this recognition can be considered as "transformed cell pattern recognition" by NK cells, similar to pattern recognition of infectious agents employed by the innate immune system in which NK cells play a central role.

In conclusion, we showed that NKp44 binds to tumor cells in a HSPGs-dependent manner and characterized the amino acids implicated in this recognition. Our results contribute an additional piece of information for the identity of the cellular ligands recognized by NCRs.

ACKNOWLEDGMENT

We thank Dr. Zer Hagit from the Hebrew University of Jerusalem for assistance in BIAcore studies.

SUPPORTING INFORMATION AVAILABLE

Five figures showing biochemical characterizations of NKp44-Ig and its mutants (MALDI, SDS−PAGE gels with and without β-ME). Also available is a residual figure for the BIAcore analysis. This material is available free of charge via the Internet at http://pubs.acs.org.

REFERENCES

1. Moretta, L., and Moretta, A. (2004) Unravelling natural killer cell function: triggering and inhibitory human NK receptors, *EMBO J. 23*, 255−259.
2. Moretta, A., Bottino, C., Vitale, M., Pende, D., Cantoni, C., Mingari, M. C., Biassoni, R., and Moretta, L. (2001) Activating receptors and coreceptors involved in human natural killer cell-mediated cytolysis, *Annu. Rev. Immunol. 19*, 197−223.
3. Biassoni, R., Cantoni, C., Pende, D., Sivori, S., Parolini, S., Vitale, M., Bottino, C., and Moretta, A. (2001) Human natural killer cell receptors and co-receptors, *Immunol. Rev. 181*, 203−214.
4. Bakker, A. B., Wu, J., Phillips, J. H., and Lanier, L. L. (2000) NK cell activation: distinct stimulatory pathways counterbalancing inhibitory signals, *Hum. Immunol. 61*, 18−27.
5. Ljunggren, H. G., and Karre, K. (1990) In search of the 'missing self': MHC molecules and NK cell recognition, *Immunol. Today 11*, 237−244.
6. McQueen, K. L., and Parham, P. (2002) Variable receptors controlling activation and inhibition of NK cells, *Curr. Opin. Immunol. 14*, 615−621.
7. Braud, V. M., and McMichael, A. J. (1999) Regulation of NK cell functions through interaction of the CD94/NKG2 receptors with the nonclassical class I molecule HLA-E, *Curr. Top. Microbiol. Immunol. 244*, 85−95.
8. Moretta, L., Bottino, C., Pende, D., Vitale, M., Mingari, M. C., and Moretta, A. (2004) Different checkpoints in human NK-cell activation, *Trends Immunol. 25*, 670−676.
9. Moretta, A., Biassoni, R., Bottino, C., Mingari, M. C., and Moretta, L. (2000) Natural cytotoxicity receptors that trigger human NK-cell-mediated cytolysis. *Immunol. Today 21*, 228−234.
10. Bloushtain, N., Qimron, U., Bar-Ilan, A., Hershkovitz, O., Gazit, R., Fima, E., Korc, M., Vlodavsky, I., Bovin, N. V., and Porgador, A. (2004) Membrane-associated heparan sulfate proteoglycans are involved in the recognition of cellular targets by NKp30 and NKp46, *J. Immunol. 173*, 2392−2401.
11. Zilka, A., Landau, G., Hershkovitz, O., Bloushtain, N., Bar-Ilan, A., Benchetrit, F., Fima, E., van Kuppevelt, T. H., Gallagher, J. T., Elgavish, S., and Porgador, A. (2005) Characterization of the heparin/heparan sulfate binding site of the natural cytotoxicity receptor NKp46, *Biochemistry 44*, 14477−14485.
12. Vieillard, V., Strominger, J. L., and Debre, P. (2005) NK cytotoxicity against CD4+ T cells during HIV-1 infection: a gp41 peptide induces the expression of an NKp44 ligand, *Proc. Natl. Acad. Sci. U.S.A. 102*, 10981−10986.
13. Cantoni, C., Ponassi, M., Biassoni, R., Conte, R., Spallarossa, A., Moretta, A., Moretta, L., Bolognesi, M., and Bordo, D. (2003) The three-dimensional structure of the human NK cell receptor NKp44, a triggering partner in natural cytotoxicity, *Structure (Camb.) 11*, 725−734.
14. Biron, C. A., and Brossay, L. (2001) NK cells and NKT cells in innate defense against viral infections, *Curr. Opin. Immunol. 13*, 458−464.
15. Cerwenka, A., and Lanier, L. L. (2001) Natural killer cells, viruses and cancer, *Nat. Rev. Immunol. 1*, 41−49.

16. Mandelboim, O., Lieberman, N., Lev, M., Paul, L., Arnon, T. I., Bushkin, Y., Davis, D. M., Strominger, J. L., Yewdell, J. W., and Porgador, A. (2001) Recognition of haemagglutinins on virus-infected cells by NKp46 activates lysis by human NK cells, *Nature 409*, 1055−1060.
17. Arnon, T. I., Lev, M., Katz, G., Chernobrov, Y., Porgador, A., and Mandelboim, O. (2001) Recognition of viral hemagglutinins by NKp44 but not by NKp30, *Eur. J. Immunol. 31*, 2680−2689.
18. Mandelboim, O., and Porgador, A. (2001) NKp46, *Int. J. Biochem. Cell Biol. 33*, 1147−1150.
19. Porgador, A., Mandelboim, O., Restifo, N. P., and Strominger, J. L. (1997) Natural killer cell lines kill autologous beta2-microglobulin-deficient melanoma cells: implications for cancer immunotherapy, *Proc. Natl. Acad. Sci. U.S.A. 94*, 13140−13145.
20. Kleeff, J., Wildi, S., Kumbasar, A., Friess, H., Lander, A. D., and Korc, M. (1999) Stable transfection of a glypican-1 antisense construct decreases tumorigenicity in PANC-1 pancreatic carcinoma cells, *Pancreas 19*, 281−288.
21. Esko, J. D. (1991) Genetic analysis of proteoglycan structure, function and metabolism, *Curr. Opin. Cell Biol. 3*, 805−816.
22. Campbell, K. S., Yusa, S., Kikuchi-Maki, A., and Catina, T. L. (2004) NKp44 triggers NK cell activation through DAP12 association that is not influenced by a putative cytoplasmic inhibitory sequence, *J. Immunol. 172*, 899−906.
23. Arnon, T. I., Achdout, H., Lieberman, N., Gazit, R., Gonen-Gross, T., Katz, G., Bar-Ilan, A., Bloushtain, N., Lev, M., Joseph, A., Kedar, E., Porgador, A., and Mandelboim, O. (2004) The mechanisms controlling the recognition of tumor and virus infected cells by NKp46, *Blood 103*, 664−672.
24. Achdout, H., Arnon, T. I., Markel, G., Gonen-Gross, T., Katz, G., Lieberman, N., Gazit, R., Joseph, A., Kedar, E., and Mandelboim, O. (2003) Enhanced recognition of human NK receptors after influenza virus infection, *J. Immunol. 171*, 915−923.
25. Dennissen, M. A., Jenniskens, G. J., Pieffers, M., Versteeg, E. M., Petitou, M., Veerkamp, J. H., and van Kuppevelt, T. H. (2002) Large, tissue-regulated domain diversity of heparan sulfates demonstrated by phage display antibodies, *J. Biol. Chem. 277*, 10982−10986.
26. Cantoni, C., Bottino, C., Vitale, M., Pessino, A., Augugliaro, R., Malaspina, A., Parolini, S., Moretta, L., Moretta, A., and Biassoni, R. (1999) NKp44, a triggering receptor involved in tumor cell lysis by activated human natural killer cells, is a novel member of the immunoglobulin superfamily, *J. Exp. Med. 189*, 787−796.
27. Bloushtain, N., Qimron, U., Bar-Ilan, A., Hershkovitz, O., Gazit, R., Fima, E., Korc, M., Vlodavsky, I., Bovin, N. V., and Porgador, A. (2004) Membrane-associated heparan sulfate proteoglycans are involved in the recognition of cellular targets by NKp30 and NKp46, *J. Immunol. 173*, 2392−2401.
28. Porgador, A. (2005) Natural cytotoxicity receptors: pattern recognition and involvement of carbohydrates, *Sci. World J. 5*, 151−154.
29. Desai, U. R., Wang, H. M., and Linhardt, R. J. (1993) Specificity studies on the heparin lyases from *Flavobacterium heparinum*, *Biochemistry 32*, 8140−8145.
30. Ornitz, D. M., and Itoh, N. (2001) Fibroblast growth factors, *Genome Biol. 2*, 1−12.
31. Capila, I., and Linhardt, R. J. (2002) Heparin-protein interactions, *Angew. Chem., Int. Ed. 41*, 391−412.
32. de Fougerolles, A. R., Batista, F., Johnsson, E., and Fearon, D. T. (2001) IgM and stromal cell-associated heparan sulfate/heparin as complement-independent ligands for CD19, *Eur. J. Immunol. 31*, 2189−2199.
33. Sugahara, K., and Kitagawa, H. (2002) Heparin and heparan sulfate biosynthesis, *IUBMB Life 54*, 163−175.
34. Garg, A., Barnes, P. F., Porgador, A., Roy, S., Wu, S., Nanda, J. S., Griffith, D. E., Girard, W. M., Rawal, N., Shetty, S., and Vankayalapati, R. (2006) Vimentin expressed on Mycobacterium tuberculosis-infected human monocytes is involved in binding to the NKp46 receptor, *J. Immunol. 177*, 6192−6198.
35. Nolte-'t Hoen, E. N., Almeida, C. R., Cohen, N. R., Nedvetzki, S., Yarwood, H., and Davis, D. M. (2007) Increased surveillance of cells in mitosis by human NK cells suggests a novel strategy for limiting tumor growth and viral replication, *Blood 109*, 670−673.
36. Warren, H. S., Jones, A. L., Freeman, C., Bettadapura, J., and Parish, C. R. (2005) Evidence that the cellular ligand for the human NK cell activation receptor NKp30 is not a heparan sulfate glycosaminoglycan, *J. Immunol. 175*, 207−212.
37. Draghi, M., Pashine, A., Sanjanwala, B., Gendzekhadze, K., Cantoni, C., Cosman, D., Moretta, A., Valiante, N. M., and Parham, P. (2007) NKp46 and NKG2D Recognition of infected dendritic cells is necessary for NK cell activation in the human response to influenza infection, *J. Immunol. 178*, 2688−2698.
38. Smetsers, T. F., van de Westerlo, E. M., ten Dam, G. B., Clarijs, R., Versteeg, E. M., van Geloof, W. L., Veerkamp, J. H., van Muijen, G. N., and van Kuppevelt, T. H. (2003) Localization and characterization of melanoma-associated glycosaminoglycans: differential expression of chondroitin and heparan sulfate epitopes in melanoma, *Cancer Res. 63*, 2965−2970.
39. Blackhall, F. H., Merry, C. L., Davies, E. J., and Jayson, G. C. (2001) Heparan sulfate proteoglycans and cancer, *Br. J. Cancer 85*, 1094−1098.
40. Jayson, G. C., Lyon, M., Paraskeva, C., Turnbull, J. E., Deakin, J. A., and Gallagher, J. T. (1998) Heparan sulfate undergoes specific structural changes during the progression from human colon adenoma to carcinoma in vitro, *J. Biol. Chem. 273*, 51−57.

BI7000455